Proceedings of IMECE2008
2008 ASME International Mechanical Engineering Congress and Exposition
October 31-November 6, 2008, Boston, Massachusetts, USA

IMECE2008-68676

FEASIBILITY OF THERMOELECTRIC WASTE HEAT RECOVERY IN LARGE SCALE SYSTEMS

Jacob LaManna[1] **David Ortiz**[1]

Mark Livelli[1] **Samuel Haas**[1] **Chinedu Chikwem**[1]

Brittany Ray[2] **Robert Stevens**[1,a]

[1] Department of Mechanical Engineering, Rochester Institute of Technology, Rochester, NY, USA
[2] Department of Industrial and Systems Engineering, Rochester Institute of Technology, Rochester, NY, USA
[a] Corresponding author email: rjseme@rit.edu

ABSTRACT

With the growing emphasis on energy efficiency because of environmental, political, and economic reasons and the fact there has been significant advances in thermoelectric materials, there is a renewed interest in using thermoelectrics for waste heat recovery. A mathematical model of a thermoelectric power system is developed from a heat transfer analysis of a waste heat recovery system. The model is validated by altering design parameters of a small prototype thermoelectric system that converts heat into electricity. A heated air stream is produced using an exhaust simulation test stand and provides the waste heat source for the prototype. The prototype is designed to be able to change several system parameters such as different heat sinks, thermoelectric module counts, and module configurations to better validate the developed model. The model does predict the electrical performance with typical accuracy of 30% error from the prototype over a range of configurations and operating conditions. A feasibility study using the validated model was used to determine under what conditions this technology will become economically viable, such as remote power generation with 20 year payback.

INTRODUCTION

In recent years, the cost of fuels has dramatically increased. With this, the world has become more concerned with the efficient use of energy. A large source of wasted energy in the form of heat occurs in turbo machinery located in an industrial setting. Some of these machines, as is the case of the VECTRA 40 gas turbine, lose 60% of the energy input as waste heat which is expelled to the atmosphere [1]. This study examines the feasibility of using thermoelectric (TE) modules to recover energy from that waste heat, ultimately increasing system efficiency. Studies of waste heat recovery with TE modules have been conducted [2, 3, 4] but have not studied the future feasibility of the technology.

Thermoelectrics are solid state devices with two basic modes of operation. The first mode, based on the Peltier Effect, requires the application of current through the module, which causes the absorption of heat from one side of the device and an expulsion from the other side. The generation of cold and hot faces of the plate makes Peltier devices ideal for heating and cooling applications. Conversely, the Seebeck Effect and second mode of operation can be used for power generation purposes. When a temperature gradient is applied across a TE module, an electric current is generated.

TE modules have been available off the shelf since the 1960's but have not been developed much on the materials end because of low efficiencies (~5%). The typical measure of efficiency for TE modules is the Figure of Merit (ZT) [5], which currently has a value around one. Figure of Merit is calculated by dividing the multiplication of the electrical conductivity and the square of the Seebeck coefficient with the thermal conductivity of the material. In the last decade, however, attention has been drawn to power generation applications due to advancement in nanostructures and semiconductor materials [6, 7]. These developments are expected to dramatically increase power generation efficiencies associated with the TE module with the Figure of Merits of new materials in the lab exceeding two and the promise of even higher values. Values of 3-4 are typically assumed to be necessary for TE modules to be competitive with current mechanical recovery systems. Improvements are still being engineered in-lab; however, industry anticipates these higher efficiency modules to become commercially available in the next five to ten years.

This research has two main objectives. The first objective is to understand how TE modules can be used in power generation and how they operate in a large scale system. The second objective is to gain insight into when technical and economic viability for waste heat recovery may occur. To meet these objectives, a system model was developed to relate an in-house exhaust simulator to the Dresser-Rand VECTRA gas turbine, a modular prototype was then built to verify the model, and the model was then refined and used to conduct a feasibility study.

NOMENCLATURE

α	module level effective Seebeck coefficient (V/K)
c_p	Specific Heat (kJ/kg)
f	inflation rate
i	prime rate
I	Electrical Current (A)
$\dot{m}$	Mass Flow Rate (kg/s)
Nmz	Number of modules per Zone
q	Heat Rate (W)
R	Resistance (Ω or K/W)
T	Temperature (K)
Z	Figure of Merit

Subscripts

1	Hot surface of module
2	Cold surface of module
3	Heat flux through insulation
c	Cold
cond2	Duct axial conduction resistance
ete	TE electrical resistance
h	Hot
i	In
ins	Insulation thermal resistance
j	j^{th} element
load	Load electrical resistance
o	out
thcz	Cold plate thermal resistance
thhz	Duct & fin thermal resistance
thte	TE thermal resistance

HEAT TRANSFER MODEL

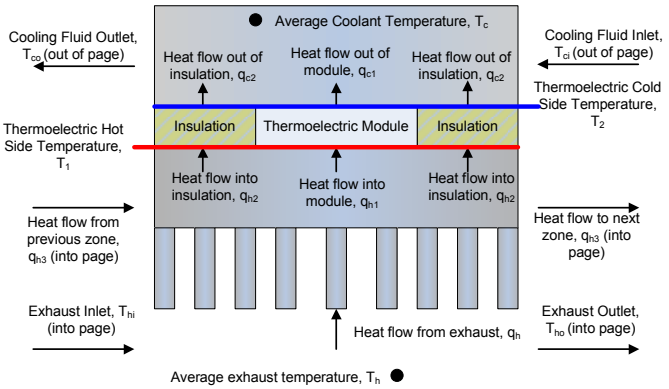

Figure 1: Visualization of thermal model

The accurate prediction of temperature distribution and therefore power generation of a hypothetical thermoelectric waste heat recovery system requires that a physical model be developed which accounts for the two-dimensional transfer of heat within the prescribed system (Fig. 1).

All surfaces, although each at a unique temperature, are considered to be isothermal. It must be recognized that a true temperature distribution across material surfaces does in fact exist, however, for the simplification of analysis and purpose to conduct a preliminary feasibility study; such an effect has been neglected. The model also assumes that the sides of the duct are taken to be perfectly insulated. By insulating the exposed surfaces of the duct exterior, the heat transfer rate through this third dimension is much smaller than that through the thermoelectric modules themselves, and thus its absence from the calculation justifiable. With this in mind, the first set of equations averages the inlet and outlet temperatures of the exhaust and coolant fluids within a particular zone.

$$T_{h(j)} = \frac{T_{hi(j)} + T_{ho(j)}}{2} \tag{1}$$

$$T_{c(j)} = \frac{T_{ci(j)} + T_{co(j)}}{2} \tag{2}$$

Utilizing the method of electrical analogy, expressions for the hot and cold surface temperatures of the thermoelectric modules are derived. These equations equate the total heat flux transferred through the duct and fin material into the modules (or that transferred through the cold plate material into the cooling fluid), solving for the particular surface temperature of interest.

$$T_{1(j)} = T_{h(j)} - N_{mz} q_h R_{thhz} \tag{3}$$

$$T_{2(j)} = T_{c(j)} + N_{mz} q_{c(j)} R_{thcz} \tag{4}$$

The thermal properties and flow conditions of the exhaust gas and cooling fluid allow for the calculation of the exhaust outlet temperature and hypothetical coolant inlet temperature. This is achieved by relating the thermal capacity of the fluid through temperature drop and specific heat to the corresponding heat flux either entering or leaving the modules.

$$T_{ho(j)} = T_{hi(j)} - \frac{N_{mz} q_{h(j)}}{\dot{m}_h c_{p,h}} \tag{5}$$

$$T_{ci(j)} = T_{co(j)} - \frac{N_{mz} q_{c(j)}}{\dot{m}_c c_{p,c}} \tag{6}$$

With the knowledge of the exhaust gas inlet temperature to a particular zone, the outlet temperature becomes available. However, by the nature of the counter flow heat exchanger, at the start of the calculation neither the inlet nor outlet temperature of the cooling fluid is known. This calculation

requires a Kludge method, for which an initial guess for the outlet temperature is established and adjusted continuously until the proper inlet temperature is achieved.

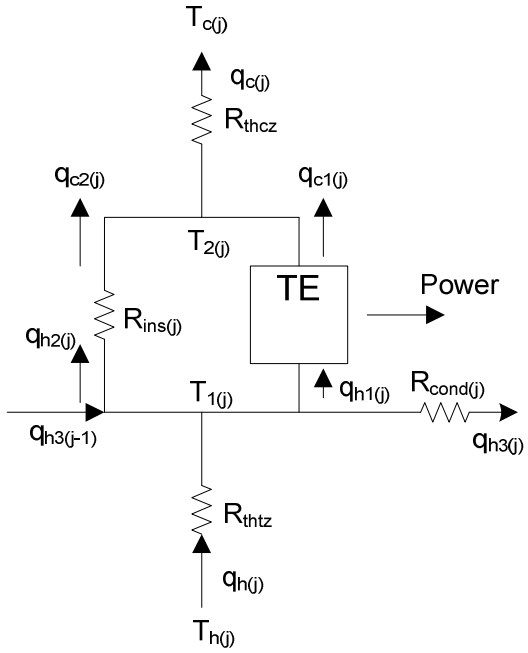

Figure 2: Thermal resistance circuit from exhaust air to cooling water

By analysis of the thermal circuit presented in Fig. 2, it becomes apparent that

$$q_{h(j)} = q_{h1(j)} + q_{h2(j)} + q_{h3(j)} - q_{h3(j-1)} \tag{7}$$

$$q_{h2(j)} = \frac{T_{1(j)} - T_{2(j)}}{R_{ins}} \tag{8}$$

$$q_{h3(j)} = \frac{T_{1(j)} - T_{1(j+1)}}{R_{cond\,2}} \tag{9}$$

$$q_{c(j)} = q_{c1(j)} + q_{h2(j)} \tag{10}$$

The following equations, based on the properties of the thermoelectrics themselves and developed from Eqn. 8 and 9, relate the thermal properties of the system to the electrical generation of the modules.

$$q_{h1(j)} = \frac{T_{1(j)} - T_{2(j)}}{R_{thte}} - \frac{1}{2} I_j^2 R_{ete} + \alpha T_{1(j)} I_{(j)} \tag{11}$$

$$q_{c1(j)} = \frac{T_{1(j)} - T_{2(j)}}{R_{thte}} + \frac{1}{2} I_j^2 R_{ete} + \alpha T_{1(j)} I_{(j)} \tag{12}$$

$$I_j = \frac{\alpha\left(T_{1(j)} - T_{2(j)}\right)}{R_{ete} + R_{load}} \tag{13}$$

It should be noted that the above governing set of equations has produced thirteen equations with fourteen unknowns for each zone. However, for the first zone calculation, the secondary dimension heat flux received into the zone may be neglected, as there is no duct material preceding the zone from which a transfer of thermal energy may occur. Thus, each iterative set of equations within a zone is well posed and solvable.

The solution to this equation set is accomplished through a Gauss-Jordan iterative process using Matlab® software, from which the temperature distributions and power generation are plotted for each respective zone of the thermoelectric waste heat recovery system. Fig. 3 displays a graphical representation of the model output, illustrating the trend and effect of fin quantity with respect to the current and power generated. The above figure also offers insight to the effect of multiple module zones, allowing the user to determine when current or power generation drops below a predetermined value, making the addition no longer a benefit to the system.

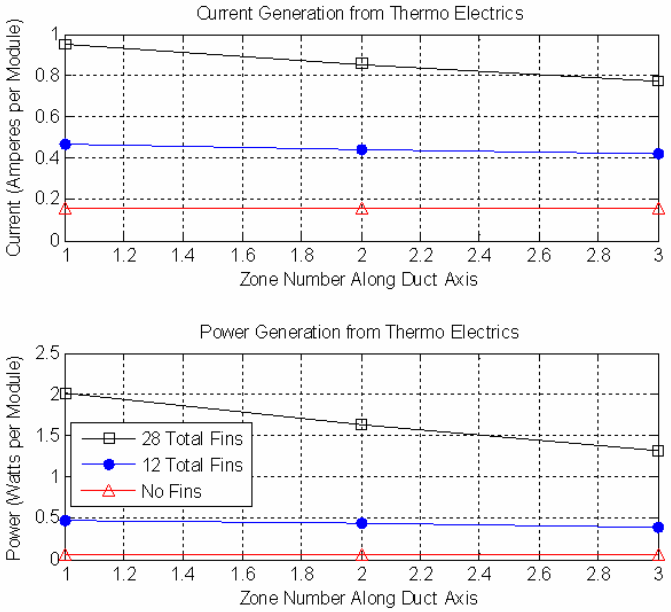

Figure 3: Model output for 8 Melcor modules per zone at 200°C and 0.043 m^3/s.

PROTOTYPE / FABRICATION

A modular prototype was designed to enable various test configurations to verify the above analytical heat transfer model. The ability to vary the number and type of TE modules, geometry of the fins, and exhaust flow rates and temperatures was critical to the design of the prototype. The prototype is comprised of four main components, the duct, the TE modules, the cold plate, and the compression plate and is constructed primarily out of aluminum to increase conduction through the duct wall to the TE modules.

The exhaust duct of the prototype is broken into three distinct zones to mitigate isothermal effects and provide insight on how temperature changes down the length of the duct. To

exaggerate the temperature gradients down the length of the duct, insulation is placed between the mating surfaces of each segment. Each segment is also broken in half to allow easy access and swap out of the internal heat sinks and provide a compressive force minimizing contact resistances of the fins to the duct. The different fin inserts are mated to the inside of each duct segment half with a dovetail joint. The duct sections in a fully assemble state with the fins removed in an exploded view can be seen in Fig. 4.

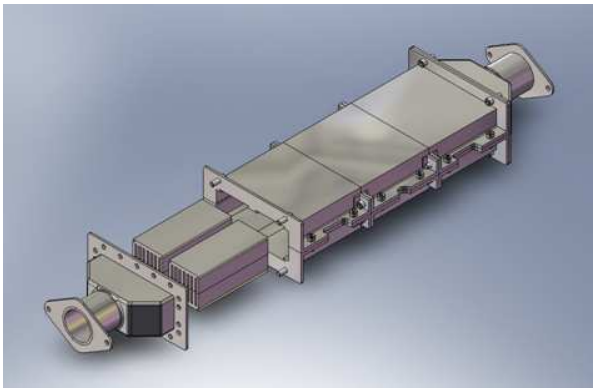

Figure 4: Segmented duct assembly with three zones (compression/cold plates are not shown)

Three brands of TE modules were selected for use on the prototype. Twelve Tellurex G1-1.4-127-1.14 modules, 24 Melcor HT8-12-40 modules, and 6 Hi-Z HZ14 modules were selected to allow for module layout variance and module property variance, a summery of module properties is given in Table 1. The thermoelectrics are mounted on the face of the duct using a highly conductive thermal paste to minimize contact resistances at the interface. The modules in each zone are wired in series with the other modules in that zone.

Table 1: Thermoelectric module properties

	Melcor	Hi-Z	Tellurex
Power Max [W]	3.3	13	5.6
Current Max [A]	1.2	8	1.5
Voltage Max [V]	2.8	1.65	3.7
Internal Resistance [Ω]	2.3	0.15	2.66

Cold plates were the selected method for cooling because of the heat removal properties of water. The maximum temperature gradient possible across the TE module was desired so a liquid cooling system was selected to achieve the highest rate and most controllable source of cooling possible. Two cold plates were implemented in the prototype, one for each face of the duct, and are connected in parallel with each other. The cold plates also distribute the compressive force across the TE modules.

The final major component of the prototype is the compression plates. These plates provide the compressive force required to minimize contact resistance on the module faces. The modules are rated at 175 to 300psi of compression force for optimal performance. Belleville disk springs are used on both ends of each compression bolt to mitigate thermal expansion effects on pressure of the duct on the TE modules. The assembly is supported by a set of jacks to relieve misalignment and pressure variations that would be induced by bending stresses.

Thirty-four thermocouples are mounted at various critical locations along the duct to provide data to be compared to the analytical model. Sixteen thermocouple probes are mounted in channels on the duct surface beneath the hot side face of the TE modules. The remaining thermocouples are wire thermocouples that are taped to the surface of the cold plate to measure the cold side temperature.

The prototype is mounted to the test stand with a two bolt automotive exhaust flange / end tank combination. The end tanks provide a transition from the 2 inch diameter test stand piping to the 5x2 inch rectangular duct of the prototype. An overall exploded view of the prototype showing how the Melcor modules are mounted to the duct can be seen in Fig. 5.

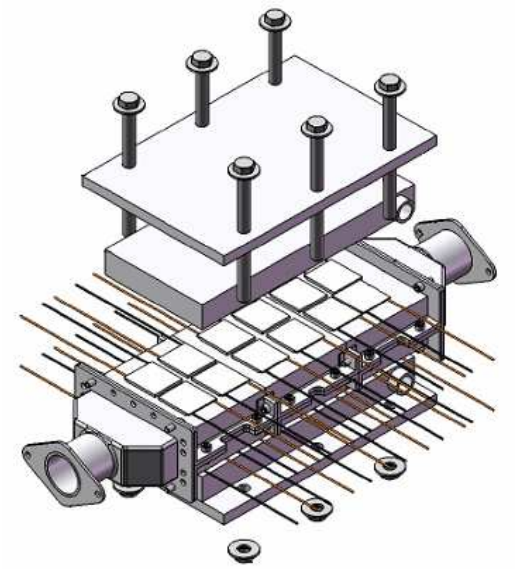

Figure 5: Complete Prototype Assembly Drawing

ELECTRICAL

For each configuration of the prototype and each flow profile, the electrical power generated by the system needs to be measured and analyzed. This is accomplished through use of a test fixture that dissipates the electrical power produced by the thermoelectric modules, through several high power rheostats, which are simply variable, wire-wound resistors.

The thermoelectric modules are distributed along the length of the prototype duct in three thermal zones. In each zone the modules are placed thermally in parallel, but electrically in series. The series circuit consisting of the thermoelectric modules in each zone is terminated by one of the rheostats in the test fixture. The voltage dropped across the rheostat as well as the value of the rheostat's resistance is recorded and used to calculate the power dissipated by the rheostat according to the following relationship:

$$P = \frac{V_T^2}{R_T} \tag{14}$$

The use of a rheostat in this application is critical, because it allows the test resistance to be changed on demand in order to match the internal impedance presented by the thermoelectric

modules in the circuit. It is important to match this impedance because that will ensure maximum power is delivered to the test load.

In order to determine the total internal impedance of the TEG modules two measurements need to be taken. The Open Circuit Voltage (OCV) of the module series circuit must be measured. Then the voltage across the test load when it is connected to the series circuit must also be measured. Using these values the unknown value of the modules' total impedance can be calculated as follows:

$$R_{Internal} = R_T \times \left(\frac{V_{OC}}{V_T} - 1 \right) \quad (15)$$

where V_{OC} is the open circuit voltage measured at the terminals of the module series. It is important to allow time for the module OCV to reach steady state before the measurement is taken as the OCV will initially increase from the time the circuit is initially opened. This time does not seem to significantly vary between module types. Therefore, the accuracy of the internal impedance measurements will depend on an accurate reading of the open circuit voltage.

TEST STAND

The test stand used to run the prototype for this project is an automotive exhaust simulation stand. Hot exhaust is simulated by blowing air through a piping system which includes a control valve, flow meter, 10kW heater, and temperature measurements. Prototype cooling water is supplied from a storage tank where it passes through temperature measurements, a flow meter, and a radiator to dump the excess heat. The test stand provides output data on the air and prototype cooling water flow rates, air temperatures before the heater, between the heater and prototype and after the prototype, and water temperatures before and after the prototype. A schematic of the test stand can be seen in Fig. 6 where the red solid lines represent the hot exhaust side and the blue dashed lines represent the cold water lines.

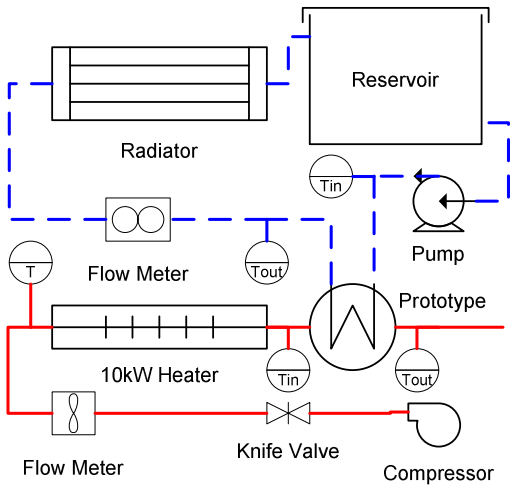

Figure 6: Test Stand Flow Schematic

TEST PROCEDURE

A test procedure was developed to provide guidance for the specific tests to be conducted for model verification. As discussed in the prototype description section, the prototype was designed to provide multiple physical configurations to give the model several points of verification. The test procedure breaks down these different configurations into three main groups with subtasks under each group.

The three main groups represent the three brands of thermoelectrics selected for testing. For each module type, three fin configurations were analyzed, 7 fin inserts (for 14 fin total), 4 fin inserts (for 8 fin total), and no fins. Each fin configuration was tested twice for each module, one test to vary temperature with constant flow rate and the second to vary flow rate with constant temperature. The 14 fin total configuration is represented by the 28 fin configuration in the model. Doubling the number of fins in the model is to account for heat traveling symmetrically from the center of the fins to the outside surface of the duct.

Testing began once the prototype has been assembled into the desired configuration and installed into the test stand. From this point the flow conditions were set and the temperature was ramped up slowly to the test point to avoid damaging the heater. Once the test stand and prototype reached steady state, data was collected using a custom LabVIEW™ GUI that collects 34 prototype temperature readings, five test stand temperature readings, test stand air flow rate, test stand cooling water flow rate, and the three thermoelectric zone output voltages.

RESULTS

The first configuration for the prototype tested was the 14 fin configuration. Under this configuration no modules were placed on the prototype to allow for thermal resistance (R_{thhz} and R_{thcz}) testing. This thermal resistance testing was necessary to experimentally characterize the resistance from convection from the air stream to the fins, conduction through the fins, contact resistance between the fins and the duct, and conduction through the duct. The value found experimentally was placed in the model instead of having the model calculate the convection coefficient and all of the resistances.

The first module configuration tested in the prototype was the Tellurex modules. Twelve total modules were used with four modules per zone, two modules on each half of the duct. The modules were placed side-by-side across the center of the duct with 6.4 mm gap between the modules for the first and third zones. Modules were configured differently for the second zone with the modules staggered corner to corner on a diagonal with 6.4 mm gap between module corners.

The Tellurex setup achieved an overall maximum system power output of 27.6W at 175°C and 0.043 m^3/s. An unexpected outcome for the power output was that second zone produced more power than either first or third zones with an output of 11.5W compared to 7.8W and 8.3W for the first and third zones, respectively. This higher power output is most likely due to the module configuration. In the staggered configuration the importance of heat spreading was less important so each module was able to have a greater heat flux and hot side temperature compared to the configuration where the modules were more closely packed.

The second module configuration tested was the Melcor modules. Twenty four modules were used with eight modules per zone and four modules per face. The modules were arranged in a 2x2 square pattern on each zone face with 3.2 mm spacing gaps between modules.

The Melcor tests achieved the highest power output for the prototype. Power output that was actually measured was 51.9W at 200°C and 0.043 m^3/s. This output was actual power not maximum power output for the configuration due to the inability to match loads. The rheostats used to dissipate the produced power were undersized because initially it was thought that the modules would be connected in a parallel and series combination in each zone thus lowering the resistance in each zone. It was decided not to run the parallel/series combination as this could result in back feed if one parallel leg was at a lower voltage than the other. This would then result in lower power output and lower system efficiencies. The internal impedance and open circuit voltage for each zone was used to extrapolate out to the maximum power. It was found that the ideal maximum power output under the given test conditions would be 60.4W.

The last module configuration to be tested was the Hi-Z modules. Six modules were used for this configuration due to the significantly larger size of the Hi-Z modules when compared to the Melcor or Tellurex, one module per face of a zone for a total of two modules per zone. The first and third zones had the modules located close to the connection joint to the second zone to keep the modules under the cold plates.

The Hi-Z modules achieved the lowest power output of the three configurations with a total power output of 20.0W at 200°C and 0.043 m^3/s. The power output of each module is significantly below the 14W rated power output for the modules. The reason for this is the 14W maximum output rating is achieved at a hot side temperature of 240°C while the hot side temperature of the module during the test was 140°C. The discrepancy between the test temperature of 200°C and the actual measured hot side temperature of 140°C is due to thermal resistance. The test temperature is the temperature of the hot exhaust air entering the prototype and does not actually represent the temperature of the TE surface.

The results of the experimental testing can be seen in Table 2. The data in Table 2 is broken down such that the power for each module type is displayed for each zone on the prototype in addition to the overall power for that particular test case. The power results for the Melcor modules are listed under two difference headings, actual and matched. The actual power is the dissipated power measured across the rheostat while the matched power was calculated using the calculated internal impedance. This was necessary as the rheostats could not provide enough voltage drop to match the internal resistance of the modules. To verify that the internal impedance power calculation method was accurate, all three rheostats were wired in series to provide enough resistance to match the modules which demonstrated the method was consistent with the experimental procedure.

The temperature of the air could not be raised any higher due to several limiting factors. The first limiting factor was that the test stand is not capable of heating the air stream much beyond 210°C at 0.043 m^3/s because the heater is limited to 10kW. In order to achieve higher temperatures with the test stand it would be necessary to lower the air flow rate but at the expense of reducing the convective coefficient. Therefore less heat would be transferred and the desired temperature would still not be achieved. The second limiting factor on test stand operational temperature was the thermal paste used on the prototype for reducing contact resistance. This thermal paste is limited to continuous maximum operating temperature of 200°C.

Verification of the model began by matching the inputs to the model to one of the individual test cases. The model was then run and the outputs for power and temperature profiles were compared with the experimental data. If the model differed significantly from the experimental data the experimentally collected thermal resistance value was inputted to the model. This allowed for quantification of the error induced by the convective correlations used in the model. Results of the verification tests for the model comparing the Melcor experimental data can be viewed in Table 3. In general the model tended to under predict the actual system performance for all module type configurations.

Table 2: Experimental Results for 14 Fin Test Configuration

	125℃ (0.043 m^3/s)			150℃ (0.043 m^3/s)			200℃ (0.043 m^3/s)			200℃ (0.035 m^3/s)			200℃ (0.024 m^3/s)		
	Zone 1	Zone 2	Zone 3	Zone 1	Zone 2	Zone 3	Zone 1	Zone 2	Zone 3	Zone 1	Zone 2	Zone 3	Zone 1	Zone 2	Zone 3
Tellurex Power	N/A	N/A	N/A	N/A	N/A	N/A	7.8	11.5	8.3	7.4	10.1	7.1	5.8	7.6	5.0
Tellurex $Power_{total}$	12.2			17.8			27.6			24.6			18.4		
Melcor P_{actual}	6.5	5.1	4.3	10.2	8.3	6.8	20.9	16.7	14.3	18.8	14.7	11.8	14.3	9.5	7.4
Melcor $P_{matched}$	7.4	5.8	4.9	12.2	9.6	7.7	24.2	19.6	16.6	21.8	17.2	13.8	16.6	11.3	8.6
Melcor $P_{Total,actual}$	15.9			25.3			51.9			45.2			31.2		
Melcor $P_{Total,matched}$	18.0			29.5			60.4			52.7			36.5		
Hi-Z Power	2.1	1.6	1.5	3.5	2.9	2.5	6.7	8.0	5.3	6.0	5.9	4.5	4.6	5.0	3.0
Hi-Z $Power_{total}$	7.3			8.9			20.0			16.4			12.6		

Table 3: Model Verification Comparison Data for Melcor 14 Fin Experimental Data

	125℃ (100CFM)	150℃ (100CFM)	200℃ (100CFM)	200℃ (75CFM)	200℃ (50CFM)
$P_{total,matched}$	18.0	29.5	60.4	52.7	36.5
P_{model}	12.3	19.6	39.6	38.0	29.6
P_{total} %error	31.7	33.6	34.4	27.9	19.1

FEASIBILITY STUDY

To gain insight into the economic viability of using thermoelectrics for waste heat recovery in an industrial setting, a feasibility study was conducted based upon the Dresser Rand VECTRA Gas Turbine. The model used for the feasibility study allows for the adjustment of the module figure of merit and the number of modules incorporated in the system by altering the number of modules in a particular zone as well as the total number of zones. A separate code calculates the total cost of the system, making assumptions for initial and operating costs and projected interest rates and time value of money. With this information, the optimal number of modules to minimize cost per kWh may be projected for a particular system, as well as the necessary figure of merit to lower the average energy cost of the system below that of competitive alternatives.

For the analysis, an equation was formulated to capture the projected cost associated with implementing such a system. The total cost equation was constructed by breaking down the system cost into four main categories, then further assessing the major contributors to cost within each category. For example, modules, sensors, and power handling units were factored into material cost, heat sinks and insulation into mechanical cost, cooling pumps into operating cost, as well as tooling and shipping into miscellaneous cost.

The time value of money is based upon the concept that the dollar today is worth more than the repayment of that dollar in future years. To determine the present value cost of a system, a compounding interest equation is applied to the capital investment as well as an annuity geometric gradient series equation to the operating costs. The operating costs of the cooling pump will experience the effects of the prime borrowing interest rate and inflation of a given year, while the capital investment cost is evaluated at a fixed rate. The assumed prime, *i*, and inflation rate, *f*, are 5% and 4.25% respectively, while the combined interest and inflation rate, *i'*, is calculated to be 9.46%.

As stated above, the feasibility model also requires output parameters of the system numerical model associated with the VECTRA Gas Turbine. These parameters allow for the adjustment of the module figure of merit and the number of modules incorporated in the system by altering the number of modules in a particular zone as well as the total number of zones. From this information, an optimal configuration may be evaluated.

Once an initial capital investment has been calculated, a straight line depreciation method was chosen to spread the cost equally over the lifetime of the system. With the total cost matrix spanning twenty years, the output power of the numerical model is used to calculate yearly kilowatt hour power generation (assuming the system is run continuously throughout the entire life of the system) and the optimal system cost per kilowatt hour is established (Fig. 7). As can be seen from Fig.

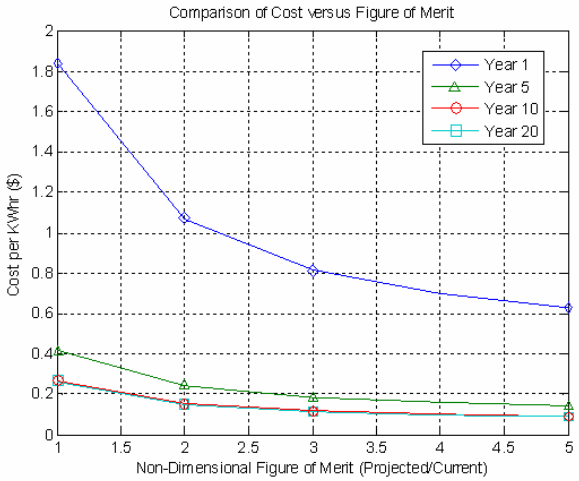

Figure 7: Graphical Comparison of Cost vs. Figure of Merit

7, based on the assumptions made, the economic viability of TE waste heat recovery systems are questionable if compared to standard electric power generation options. TE systems are potentially attractive for remote power applications where $0.10-0.20 is economically competitive. As the cost per unit power for TE modules decrease by about a factor approximately four, there is potential for TE waste heat recovery systems to compete against standard power generation technologies

CONCLUSIONS

An analytical model in addition to a physical model has been developed to gain insight into how thermoelectric modules operate in industrial systems. This insight and knowledge then lead to the development of a feasibility study to determine the payback rate and possible timeframe for when thermoelectric modules will be economically viable.

The physical model and the analytical model were able to show how heat flow from the hot exhaust gas and electrical power generation can be affected by the number of modules and configuration of modules in each zone. Modules can have a parasitic effect on neighboring modules if placed too closely. This parasitic effect will lower the hot temperature, heat flux, and ultimately the power generating potential of both modules which will have negative effects on system efficiency.

The feasibility study was able to show how module configurations and the figure of merit of a module can affect the investment costs of a thermoelectric project. As prices continue to decrease and materials improve for thermoelectric modules with an increase in current energy prices could see the advent for cost effective use of thermoelectrics in waste heat recovery. This will become feasible in applications in remote areas were the cost of energy is already much higher than typical grid prices.

ACKNOWLEDGMENTS

We would like to thank Paul Chillcott for technical advice and Dresser-Rand Corporation for financial support.

REFERENCES

[1] Personal Communication with Paul Chilcott, Dresser-Rand Corporation, paul_n_chilcott@dresser-rand.com, 716-375-3866.

[2] Haidar, J.G., and Ghojel, J.I., 2001, "Waste Heat Recovery from the Exhaust of Low-Power Diesel Engine Using Thermoelectric Generators," 20th International Conference of Thermoelectrics, Beijing, China, pp. 413-417.

[3] Crane, D.T., and Jackson, G.S., 2004, "Optimization of Cross Flow Heat Exchangers for Thermoelectric Waste Heat Recovery," Energy Conversion and Management, 45, pp. 1565-1582.

[4] Kajikawa, T., 2006, "Thermoelectric Power Generation System Recovering Industrial Waste Heat," in: D.M. Rowe (Ed.), *Thermoelectric Handbook: Macro to Nano*, CRC, pp. 50/1-27.

[5] Goldsmid, H.J., 1995, "Conversion Efficiency and Figure-of-Merit," in: D.M. Rowe (Ed.), *Thermoelectric Handbook: Macro to Nano*, CRC, pp. 3/1-25.

[6] Chen, G., Dresselhaus, M.S., Dresselhaus, G., Fleurial, J.-P., and Caillat, T., 2003, "Recent Developments in Thermoelectric Materials," International Materials Review, 48(1), pp. 45-66.

[7] Ghamaty, S., Bass, J.C., and Elsner, N.B., 2006, "Quantum Well Thermoelectric Devices and Applications," in: D.M. Rowe (Ed.), *Thermoelectric Handbook: Macro to Nano*, CRC, pp 57/1-12.

[8] Hodes, M., 2004, "One-Dimensional Analysis of Thermoelectric Modules", 2004 Inter Society Conference on Thermal Phenomena, Las Vegas, NV, USA pp. 242-250.

[9] Lineykin, S., and Ben-Yaakov, S., 2007, "Modeling and Analysis of Thermoelectric Modules," IEEE Transactions on Industrial Applications, 43(2), pp. 505-512.

[10] Ross, S.A., Westerfield, R.W., Jordan, B.D., and Jaffe, J., 2007, *Corporate Finance: Core Principles and Applications*, McGraw-Hill, New York, New York, USA.

[11] Incropera, F.P., Dewitt, D.P., Bergman, T.L., and Lavine, A.S., 2007, *Fundamentals of Heat and Mass Transfer*, John Wiley & Sons, Hoboken, New Jersey, USA.